

# INTERNATIONAL SOCIETY FOR SOIL MECHANICS AND GEOTECHNICAL ENGINEERING



*This paper was downloaded from the Online Library of the International Society for Soil Mechanics and Geotechnical Engineering (ISSMGE). The library is available here:*

<https://www.issmge.org/publications/online-library>

*This is an open-access database that archives thousands of papers published under the Auspices of the ISSMGE and maintained by the Innovation and Development Committee of ISSMGE.*

# Role of the facing on the behaviour of soil-nailed slopes under surcharge loading

## Rôle du parement sur le comportement des pentes de sol cloué sous surcharge

Sanvitale N., Simonini P., Bisson A., Cola S.

Department of Civil, Environmental and Architectural Engineering - University of Padova - Italy

**ABSTRACT:** Soil nailing is an economic and efficient method to reinforce soils, involving the insertion of threaded bars into natural unstable slope for increasing the overall stability or into cut slopes during the top-down process of excavation. The retained soil, the resisting reinforcements and the external facing are the main components of a soil-nailed structure. Their composite interactions determine the performance of soil-nail construction in terms of deformations and stability. Even if the international codes deal about the possibility of use rigid or flexible external facing, the role of facing stiffness is not sufficiently studied and evaluated. To this aim, some tests with various facing types, differing in stiffness and continuity, were carried out so far in 1g small scale physical model. The experimental results show the importance of both flexional and axial stiffness of facing in controlling the deformation of the wall during excavation and the maximum surcharge applicable at the rear of wall.

**RÉSUMÉ:** Le clouage du sol est une méthode économique et efficace pour renforcer le sol en place: il consiste en l'insertion de barres d'acier filetées ou d'autres barres dans les pentes naturelles instables ou dans des talus au cours du processus de l'excavation pour augmenter la stabilité globale. Le sol soutenu, les barres résistantes et le parement extérieur sont les principales composantes d'une structure du sol cloué. Leurs interactions mutuelles déterminent la performance du *soil nailing* en termes de déformations et de stabilité. Même si les codes internationaux considèrent la possibilité d'utiliser des parements extérieurs rigides ou flexibles, le rôle de la raideur du parement n'a pas été suffisamment étudié et évalué. Avec ce but ont été réalisées des épreuves dans un modèle physique avec des parements différents en rigidité et continuité. Les résultats expérimentaux soulignent l'importance de la raideur en flexion et en traction-compression du parement extérieur dans le contrôle de la déformation de la paroi pendant l'excavation, et la valeur maximale de la charge applicable à l'arrière du mur.

**KEYWORDS:** soil nailing, facing, retaining wall, soil reinforcement, physical model.

## 1 INTRODUCTION

Soil nailing is an economical and efficient reinforcement technique used as a remedial measure in unstable natural slopes or as retaining structure for excavated slopes. In comparison with other retaining structures, soil nailing permits to reduce the excavated soil volume, saving construction materials and realization time. Its first applications were proposed in France for the Couterre project (Plumelle et al. 1990) and in Germany (Stocker 1976). Even if many studies and researches have been already performed and several national codes or guide lines exist, the role of facing in controlling the deformation of excavated front or the slope overall stability is not completely understood yet.

On this matter, the new code EN 14490:2010 indicates the possible use of three types of facing which are:

- *hard facing* which has to fulfil the function of stabilizing the slope between the nails and shell therefore be dimensioned to sustain the maximum expected destabilizing forces;
- *flexible facing* designed to provide the necessary restrains to the areas of slope face between the bearing plates as well as the erosion control;
- *soft facing* with the primary function of controlling slope erosion in conjunction of vegetation.

Even if the EN 14490:2010 reports some examples for the three types of facing, it does not give precise indications on how to evaluate the forces applied by soil on facing or the stiffness of facing.

In order to improve the understanding of the role of facing on the resistant mechanisms of soil nailing, this paper presents

the results of an experimental program carried out on a 1g small scale physical model of sandy slope reinforced with soil nailing and brought to collapse by surcharge loading: in the tests six facings, differing for continuity and stiffness, were utilized to restrain the soil between nails.

## 2 PHYSICAL MODEL

The model face is 39.5 cm wide and 40 cm high, with a wall dip angle of 80° (Figure 1). The soil is medium-fine sand from Adige river with the following characteristics (Gottardi and Simonini 2003): mean particle diameter  $D_{50} = 0.42$  mm, non-uniformity coefficient  $C_u = D_{60}/D_{10} = 2.0$ , specific bulk weight  $G_s = 2.71$ , minimum and maximum dry specific weight  $\gamma_{d,min} = 13.6$  kN/m<sup>3</sup> and  $\gamma_{d,max} = 16.5$  kN/m<sup>3</sup>, peak friction angle  $\phi_{peak} = 42-43^\circ$  and critical friction angle  $\phi_{crit} = 35^\circ$ .

The sand is prepared in homogeneous layers into a caisson with pluvial deposition method reaching a relative density of about 85%. During deposition the caisson is maintained inclined at 20° to deposit homogeneously the sand also at rear of facing and to simplify the nail installation. In the meanwhile, the cover is fixedly bonded in vertical position, using four wooden blocks behind which will be subsequently removed to simulate the excavation.

The deposition is temporarily stopped to install the nails in 4 horizontal lines and 3 vertical lines, with spacing  $s_v = 10.2$  cm and  $s_h = 13.2$  cm respectively.

The nails are 32.5 cm long aluminium tubes, with an external diameter of 6 mm and covered with 1 mm thick layer of glued Adige sand. They are perpendicularly connected to the

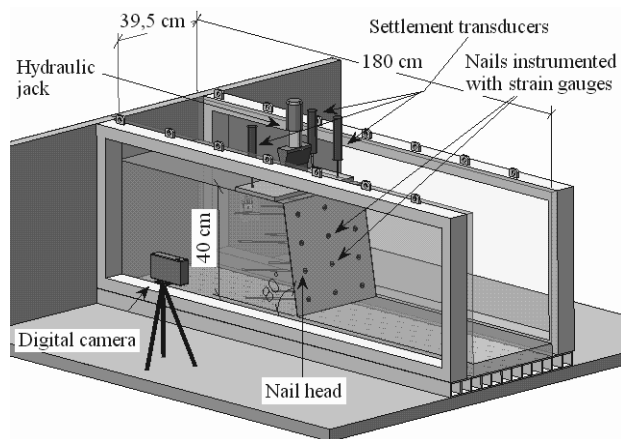


Figure 1 Perspective view of 1g physical model.

facing with a 1.2 cm annular rod and a small steel pin.

The monitoring system includes:

- A load cell between to the vertical jack and the plate to measure the load;
- Three vertical displacement transducers recording the plate settlements;
- A digital camera taking lateral images of the model during the entire test. By applying the Particle Image Velocimetry (PIV) technique (White et al. 2003) to the image sequences it is possible to reconstruct the evolution of displacement during the test;
- A laser scanner for monitoring the frontal displacement of the face at some significant load steps. Since the scanner takes about 1 min to complete the scansion, the loading sequence must be temporarily stopped. A small load reduction, due to the occurrence of the soil viscous strains, was observed in this short time interval;
- Eight strain gauges, glued pair by pair, at 2.3, 10.4, 18.5 and 26.7 cm from the face, on the nails located along the central vertical section at 15.3 and 25.4 cm from the top (the central ones). They permit to reconstruct the distribution of axial strain and, consequently, of axial stress along nails.

In order to evaluate which stiffness – i.e. the axial or the flexional ones - mostly influences the soil nailing behaviour during excavation and subsequent plate loading, six tests were performed with different facing types (Table 1 summarises the geometrical and mechanical properties of the various coverings). Four facings, covering the entire excavated front, were: *a*) 4 mm-thick plate of Polymethyl methacrylate (PMMA); *b*) a 0.25 mm-thick sheet of brass (BRASS); *c*) a steel mesh formed by 1-mm wires, perpendicularly welded at 6 mm spacing (MESH); *d*) a steel net formed by 0.24 mm-diameter wires, perpendicularly woven (NET). Three of these continuous coverings have an axial stiffness with the same order of

magnitude but a flexional stiffness decreasing about one order from one to another facing, while the fourth is very deformable both in axial and flexional sense.

The other ones are two discontinuous facing constituted by rectangular tiles in PMMA (obtained by cutting a PMMA cover like that used in test *a*): in these cases the covering ratio, defined as the ratio between the total covered area and the total extension of facing, are respectively equal to 95% (PMMA95) and 25% (PMMA25). Due to this discontinuity the axial stiffness vanishes, so these covers are flexional stiff (like the test *a*) but without any axial stiffness.

Since the soil forming the model is dry sand without cohesion, to avoid the collapse of sand among the tiles or across the mesh holes, a very light and low-resistant geo-synthetic behind them was set up. The same geo-synthetic was also inserted at the rear of the other facings to reach homogeneous test conditions.

After the models being completely set up, they were driven to failure in three steps: 1) application of a uniform load  $q$  of 24 kPa on the plate; 2) removing one by one of four wooden blocks, simulating the front excavation; 3) application of an increasing uniform load on the plate up to failure.

### 3 MODEL RESPONSE DURING EXCAVATION

Figure 2 depicts the vertical displacements of the plate,  $\Delta y_p$ , during the 4 steps of excavations in the all the tests. Even if the plate horizontal displacements,  $\Delta x_p$ , (obtained from the PIV analysis of digital images) are not reported here for brevity, they show a similar trend with the same magnitude order of vertical settlements – i.e.  $\Delta y_p/\Delta x_p \approx 1$ . Moreover, since the plate is located just at the rear of facing, the horizontal plate displacement may be considered equal to the horizontal displacement of the front tip.

Note that the vertical displacement does not exceed 0.5 mm (equivalent to 0.13% of the slope height) in tests *a* and *b* with very rigid facings (PMMA and MESH), while the maximum displacement, equal to about 2 mm and equivalent to 0.5% of the height, is observed in the tests *d* and *e* with very deformable facing (NET and PMMA25).

It is also interesting to observe that in the test with PMMA95, with discontinuous covering, the displacement does not exceed the 0.27% of the height: this means that the high flexional stiffness of PMMA tiles prevents the soil near to the face to move laterally.

Figure 3 reports the tensile force distribution along the monitored nails at the end of the excavation. Even if the tensile force is determined in few points, it is possible to recognize the typical bell-shaped distribution observed in many applications and described in the international practical guides (i.e. FWHA 2003, Geoguide7 2008). As known, the slope of the lateral segments depends on the shear stresses mobilized at the interface soil-nail in the active and passive zone respectively.

Table 1. Mechanical characteristics of facings adopted in the physical model.

Model	Facing	Covering ratio (%)	Thickness/ Wire Diam. (mm)	Wire spacing (mm)	Young modulus E (GPa)	Axial stiffness EA/m (N/mm)	Flexional stiffness EJ/m (Nmm <sup>2</sup> /mm)
a	PMMA	100	4	-	3.2	12800	17066.67
b	MESH	100	1	6	210	26180	3318.06
c	BRASS	100	0.25	-	126	31500	236.25
d	NET	100	0.24	1.02	70	3105*	22.66
e	PMMA95	95	4	-	3.2	-	-
f	PMMA25	25	4	-	3.2	-	-

\* The axial stiffness of canvas is the mean values obtained from to traction tests performed on two 178mm x 25mm samples.

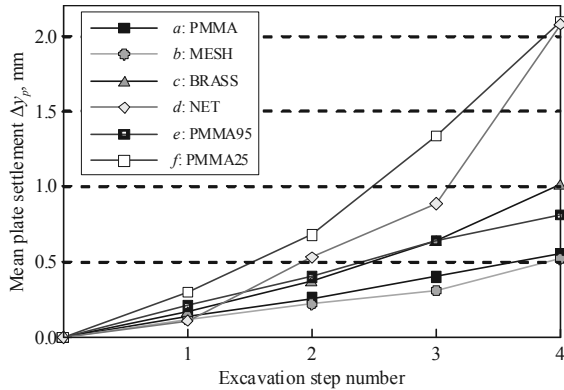


Figure 2. Average plate vertical displacement during four excavation steps in all the tests.

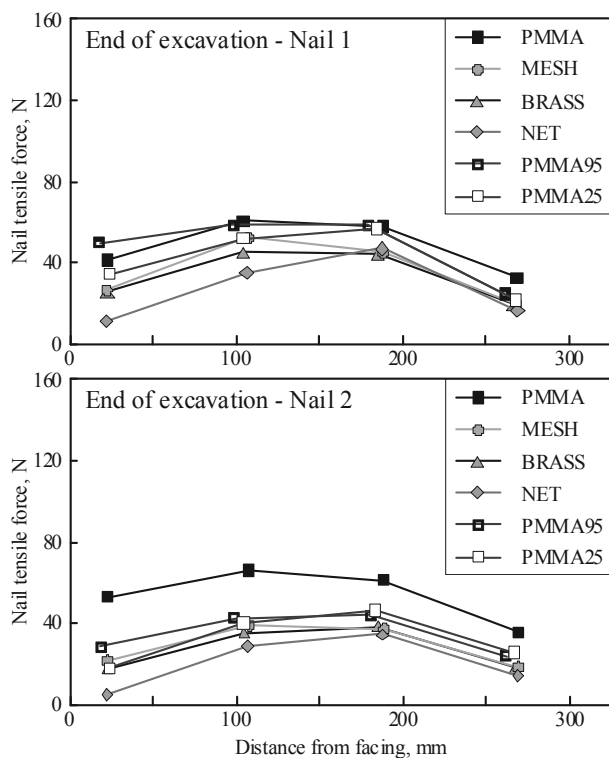


Figure 3. Distribution of tensile force along the monitored nails at the end of excavation: (a) upper nail; (b) lower nail.

The stiffness of facing strongly influences the characteristics of tensile force distribution, such as the slope of two lateral segments, the tensile force at the connection with facing,  $N_{head}$ , and the location  $X_{max}$  of maximum traction,  $N_{max}$ .

The highest  $N_{head}$  is reached in tests *a* and *e* (PMMA and PMMA95), with  $N_{head}$  gradually decreasing according to the facing deformability: the lowest values are due to tests with NET and PMMA25. On other hand, the difference  $N_{max} - N_{head}$  and consequently the slope of segment in the active zone, is less for tests with PMMA and PMMA95, gradually increasing with facing deformability. Finally,  $X_{max}$  is located closer to the face in tests with PMMA and PMMA95, while it moves itself from face using deformable covering (NET and PMMA25).

This means that if a rigid facing prevents the soil behind the face to dilate, limiting, as previously explained, the face horizontal displacements. In addition it also reduces the relative soil-nail displacement in the active zone and the increase of shear stress mobilized at this interface. On the contrary, to reduce the face deformation, the nails have to be more stressed by higher soil pressure acting at the rear of facing, because the

soil could not reach the active state condition with the mobilization of the minimum horizontal stress.

#### 4 MODEL RESPONSE DURING PLATE LOADING

Figure 4 plots the load applied to the plate during the phase *c* vs. the mean vertical displacements of the plate. Temporary reductions of the load are evident in the graph and they are due to the temporary stops of loading piston for performing the laser scanner of the front.

Figure 5 compares the spatial distribution of the cumulated shear strains at collapse in tests with PMMA, NET and PMMA25 (for brevity we choose only the most meaningful images): the shear strain distribution is determined by applying the PIV analysis to the lateral images of models.

In all the model tests, failure appears to be combined with localization of shear strain along one or more narrow bands. The mostly well-defined band moves from the plate edge (the one opposite to the face) towards the face base intercepting all the nails and delimiting the wedge pushing on facing: the wedge is characterized by a size related with the maximum load reached in the test: the greater is the maximum load, the larger is the wedge. Other bands, less clear, individuate a wedge like those that typically form below shallow foundations.

Figure 6 plots the distribution of tensile force along the monitored nails when a load of 5,45 kN is applied on the plate: note that at this load level the model *d* is approaching the collapse, and some problems affect the strain-gauge readings (localization of plastic strain in nail n.1 and detachment of one strain-gauge in nail n.2) and the correct evaluation of tension value. Moreover, data from test PMMA95 are not reported in Figure 6, because some problems occurred in the electrical connections induce to consider them not reliable.

These results permit to point out the important role played by the facing. The maximum load supported by the retaining system with rigid facing PMMA,  $P_{max,a}$ , is about five times greater than the load supported in test with NET,  $P_{max,d}$ , that represents the minimum load measured in all the tests. Other models support loads in the range  $0.83-0.97P_{max,a}$  with higher values in tests with MESH and PMMA95, the most rigid covers.

From the comparison suggested in Figure 6 it is evident that the collapse of model *d* is due to the overcoming of the pull-out resistance in the passive zone of soils. The relative soil-nail displacements, cumulated in the active zone as consequence of facing buckling, induced the increase of tensile gradient in the section of nails close to the face. Consequently, also the maximum traction increases significantly:  $N_{max}$  in test *d* is 3-4 times greater than that determined in all other tests. This high tensile force has to be compensated by the frictional resistance along the nails in the passive zone. This is evident from Figure 6, because the slopes of the tensile profile in the most internal part of the nails are greater than those characterizing the results

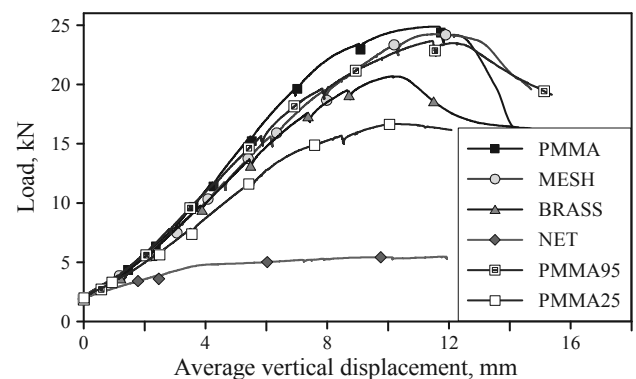


Figure 4. Load on the plate vs. mean settlements during loading phase up to collapse.

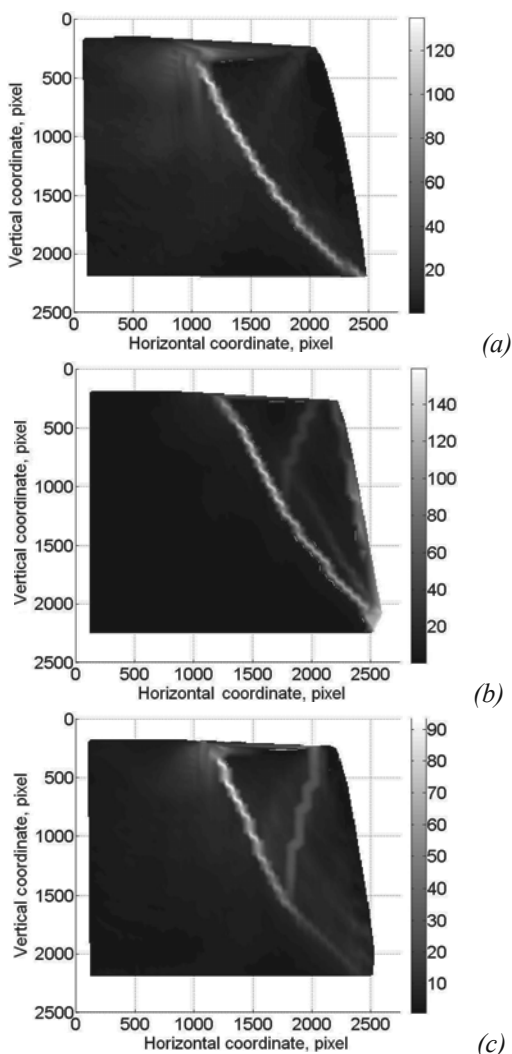


Figure 5. Total shear strain distribution at the face collapse, determined by mean of PIV in tests with PMMA (a), NET (b) and PMMA25 (c).

of other tests. It is important to note that the points marked by an asterisk in Figure 6 are largely overestimated, because approaching the failure the nails underwent to large and concentrated flexional plastic strains, also for the presence of rupture wedge of shallow foundation, and, in this strain state the relationship strain-stress is not linear yet.

Of course the tensile force distributions along nails for all the tests at failure are similar to those recorded for model *d*, even if they are not here reported for sake of brevity.

### 5 FINAL REMARKS

From the experimental results discussed above it is possible to observe that both flexional and axial stiffness influence the performance of a soil nailing system in excavation and at collapse. If the facing has no continuity, its flexional stiffness can hinder the front deformation during excavation, thus limiting the mobilization of shear stress along nails. In addition, if the facing is flexionally deformable but characterized by low axial deformability, horizontal displacements of the front too can be controlled. In both of the cases, at the end of excavation, the system has still a high level of safety in relation to the global stability problem. On the contrary, the largest deformations accumulated with excavation can reduce the safety margin.

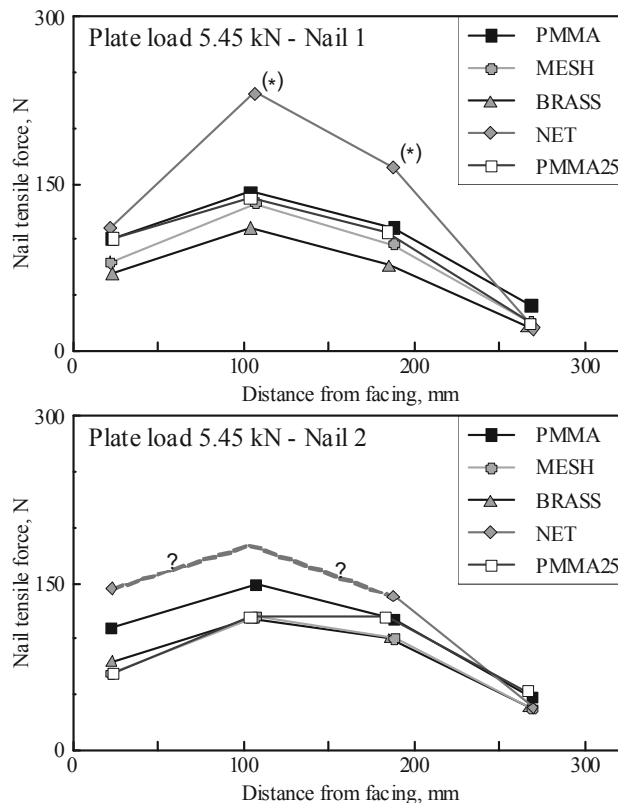


Figure 6. Distribution of tensile force along the monitored nails when the load on plate is equal to 5.45 kN (collapse load of test with NET): (a) upper nail; (b) lower nail. Notes: 1) the tensile data indicated with asterisk (\*) are determined from strain-gauge readings at a load of 5.30 kN because at greater loads the nails experimented plastic strains in these positions; 2) The trends indicated with (?) are only presumed, not measured, due to the detachment of the 2<sup>nd</sup> strain-gauge.

### 6 ACKNOWLEDGEMENTS

We want to thank the Dalla Gassa s.r.l. (Cornedo Vicentino, Italy), which sponsor this research, and Dr. D.Pilotto and M.Miuzzi for the valuable help given in the experimental tests.

### 7 REFERENCES

Geoguide7, 2008. *Guide to Soil Nail design and construction*. Geotechnical Engineering Office, Hong Kong.  
 Gottardi G., Simonini P., 2003. The viscoplastic behaviour of a geogrid-reinforced model wall. *Geosynthetics International*, 10: 34-46. ISSN: 1072-6349, doi: 10.1680/gein.2003.10.1.34.  
 EN 14490:2010: *Execution of special geotechnical works — Soil nailing*.  
 FHWA-IF-03-017, 2003. *Geotechnical Engineering circular No. 7 – Soil Nail Walls*.  
 Plumelle C., Schlosser F., Oclage P. and Knochenmus G., 1990. French national research project on Soil Nailing: CLOUTERRE, *Geotechnical Special Publication ASCE*, 25, 660-675.  
 Stocker M., 1976. Bodenvernagelung, Vorträge der Baugrundtagung, Nürnberg, *Deutsche Gesellschaft für Erd- und Grundbau e.v.*, Essen.  
 White, D.J., Take, W.A. & Bolton, M.D. 2003. Soil deformation measurement using particle image velocimetry (PIV) and photogrammetry, *Géotechnique* 53(7): 619-631.